Journal of Applied Electrochemistry **29**: 995–1003, 1999.

Surface treatment for zinc corrosion protection by a new organic chelating reagent

S. MANOV[1], F. NOLI[1]**, A.M. LAMAZOUERE[2] and L. ARIES[1]*
[1]*Laboratoire des Interfaces et Matériaux, ENSCT, 118 route de Narbonne, 31077 Toulouse cedex 4, France*
[2]*LCMIE, Université Paul Sabatier, 118 route de Narbonne, 31062 Toulouse cedex, France*
*(*author for correspondence, e-mail: aries@ramses.ups-tlse.fr)*
*(**present address: Laboratory of Radio-Chemistry, Department of General and Inorganic Chemistry, Aristotle University of Thessaloniki, 54006 Thessaloniki, Greece)*

Received 10 June 1998; accepted in revised form 26 January 1999

Key words: chelating reagent, corrosion protection, inhibitor, organometallic layer, polarization curves, surface analysis, surface treatment, zinc

Abstract

The effect on the corrosion behaviour of zinc of a new organic molecule with chelating groups was investigated. Electrochemical studies of the zinc specimens were performed in aqueous sulfate–chloride solution (0.2 M Na_2SO_4 + 0.2 M NaCl, pH 5.6) using potentiostatic polarization techniques with a rotating disk electrode. Zinc samples, previously treated by immersion in the inhibiting organic solution, presented good corrosion resistance. The influence of the treatment bath pH and temperature on the protection efficiency has been emphasized. The recorded electrochemical data indicated a basic modification of the cathodic corrosion behaviour of the treated zinc resulting in a decrease of the electron transfer rate. Corrosion protection could be explained by a chelation reaction between zinc and organic molecules and the consequent growth of an organometallic layer strongly attached to the metal surface which prevented the formation of porous corrosion products in the chloride-sulfate medium. This protective film was studied using several surface analysis techniques such as X-ray photoelectron spectroscopy (XPS), scanning electron microscopy (SEM–EDS) and Fourier transform infrared spectroscopy (FTIR).

1. Introduction

Zinc is a metal with numerous industrial applications and is mainly used for the corrosion protection of steels. In moist atmospheres zinc corrodes forming white corrosion products (white rust). Chromate solutions have been applied successfully in order to protect the zinc, but recent environmental restrictions require the chromate solutions to be replaced with other reagents. Some authors have proposed soluble salts of rare earth metals such as cerium, nickel or bismuth salts [1, 2] for white rust prevention.

Organic reagents [3–14] also provide effective corrosion inhibition. Chelating agents have shown particular promise in this field [15–18]. These substances form stable, almost insoluble metal chelates or metal complexes which act as protective coatings. In the literature the number of papers dealing with chelation agents is limited. One of the few authors working on zinc chelation is Leroy [19–22] who found several organic molecules suitable to inhibit zinc corrosion.

In this work a new organic chelating reagent is proposed (Figure 1). The synthesized molecule contains covalent (>NH) and coordinating (=S and =N—) groups in order to form a ring complex with zinc and a hydrophobic ring oriented to the environment which protects the zinc surface against corrosion. The effect of this molecule was studied in aqueous solutions using potentiostatic techniques with a rotating electrode. Emphasis was given to the investigation of the mechanism of corrosion inhibition by chelation. The protective layers formed on the zinc surface after immersion in the treatment solutions were analysed by X-ray photoelectron spectroscopy (XPS), Fourier transform infrared spectroscopy (FTIR) and scanning electron microscopy combined with energy dispersive spectroscopy (SEM–EDS).

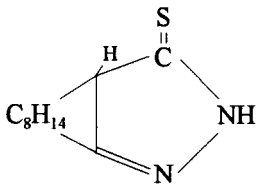

Fig. 1. Structure of the organic molecule CSN5.

2. Experimental details

2.1. *Inhibitor and test materials*

The organic molecule CSN5 used in this study contains the chelating 5-thioxo 4-hydro 1H-pyrazole group and a hydrophobic cyclic part (Figure 1).

Commercial zinc sheet (thickness 0.7 mm and composition Cu 0.17%, Ti 0.075%, Al < 0.005%, Pb–Cd < 0.003%, Fe 0.002%, Sn 0.001%, Mg 0.0005%) was cut into 1 cm^2 discs. The samples were mechanically polished using SiC paper of successive grades from 180 to 4000 then rinsed with ethanol and distilled water.

The treatment solutions were prepared by dissolving 2% ($C_M = 9.6 \times 10^{-2}$ M) or 5% ($C_M = 2.4 \times 10^{-1}$ M) of the organic molecule in 96% ethanol. The pH of the CSN5 solutions was 4.1. For the tests at different pH values, pH adjustment was carried out with HCl or NaOH. The treatment of zinc specimens was achieved by dipping in CSN5 solutions for variable immersion times and at different treatment bath temperatures. After that, the samples were rinsed once more with ethanol, washed with distilled water and dried in air.

2.2. *Electrochemical investigation*

Electrochemical experiments were performed in aerated aqueous solution of 0.2 M Na_2SO_4 + 0.2 M NaCl, pH 5.6 at 25 °C by means of a potentiostatic technique. Polarization curves were obtained using a Schlumberger–Solartron electrochemical apparatus. The cell contained a saturated calomel reference electrode (SCE), a platinum disc of 1 cm^2 area as counter electrode and the rotating working electrode (zinc specimen). The rotation rate was 1000 rpm and the potential scan rate was 20 mV for every 3 min. The cathodic and anodic curves were recorded separately starting from the free corrosion potential after a 30 min preliminary hold time.

2.3. *Surface analysis*

The surface morphology of the samples, after immersion in the CSN5 solutions and after the electrochemical test, was investigated by scanning electron microscopy using a SEM–EDS Jeol JSM 6400 microscope.

Fourier transform infrared spectroscopy (FTIR), by reflection as well as by transmission, was also applied using a Perkin–Elmer FT 1600 infrared spectrometer. An Escalab MKII VG Scientific spectrometer was used for the XPS experiments. It was equipped with an argon ions beam of 2 kV (50 μA) or 4 kV (100 μA) for sputtering and with an aluminum *K*-alpha source. The source was run at 13 kV and 300 W. The emitted photoelectrons were sampled from 10 mm^2 area.

3. Results and discussion

3.1. *Electrochemical investigation*

The polarization curve of the untreated zinc sample is presented in Figure 2. The corrosion potential (E_{corr}) was found to be −1045 mV. In the anodic region the current density increases rapidly indicating extensive dissolution of the metal. The cathodic curve exhibits two well-separated diffusion plateaus due to the dissolved oxygen reduction:

$$O_2 + 4\,e^- + 2\,H_2O \rightarrow 4\,OH^- \qquad (1)$$

The oxygen reduction mechanism becomes complex in such systems where mass transport takes place in the liquid phase as well as on the metal surface (system corrosive medium-corrosion products-metal). It is mentioned in the literature [24] that in the vicinity of the

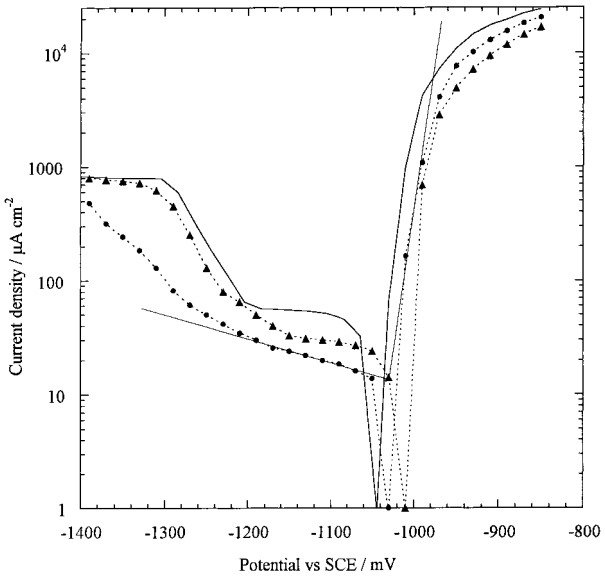

Fig. 2. Polarization curves in aerated 0.2 M Na_2SO_4 + 0.2 M NaCl aqueous solution. Solid line: untreated zinc; broken lines: treated with CSN5 zinc (2 h, 25 °C, pH 4.1). Treatment bath concentrations: (▲) 2% CSN5 and (●) 5% CSN5.

corrosion potential the oxygen reduction occurs through a more or less porous layer (first plateau). This layer consists of corrosion products and is formed during the short preliminary hold time at the free corrosion potential. At higher cathodic overpotentials (second plateau) the whole surface behaves as quasi-uniformly active, the oxygen reduction takes place at the layer-solution interface and the current density increases.

Because for untreated zinc the corrosion process in aerated sulfate solution was found to be cathodicaly controlled [24, 25], the corrosion current density can be obtained from the diffusional cathodic current at the first plateau; in the present work it was found to be 58 μA cm^{-2}.

Figure 2 also presents the polarization curves of the zinc samples treated at 25 °C for 2 h in 2% and 5% CSN5 solutions. Treatment in the solution of the organic molecule resulted in a shift of the corrosion potential (E_{corr}) towards more positive values by 15–35 mV in comparison to untreated zinc. Both the cathodic and the anodic curves were decreased. The higher corrosion resistance was exhibited by the zinc samples treated in 5% CSN5 solutions indicating that the surface exposed to the corrosive medium is less active, due to the improvement of the surface coverage by the more concentrated inhibitor. Moreover, the CSN5 treatment of the zinc samples induced a basic modification of the metal cathodic behavior. When the CSN5 concentration increased, the two typical diffusion plateaus progressively disappeared and the cathodic curve tended towards a continuous linear shape with lower current densities. This effect could result from the presence of an organometallic protective film on the electrode surface inhibiting the formation of the porous oxide layer during the preliminary hold time at the free corrosion potential and decreasing the electron transfer rate at the interface. Thus, the cathodic reaction would become substantially under charge transfer control. In this case I_{corr} was obtained by extrapolation of the linear part of the cathodic polarization curves [18].

The protection efficiency (η) was estimated to be 60% for samples treated in 2% CSN5 solution (25 °C, 2 h) and 80% for those treated in 5% CSN5 solution (25 °C, 2 h). These results were calculated using the following expression:

$$\eta = \frac{(I_{corr})_o - I_{corr}}{(I_{corr})_o} \times 100 \qquad (2)$$

where $(I_{corr})_o$ and I_{corr} denote corrosion current densities for the untreated and treated zinc, evaluated from the polarization curves. The η values are

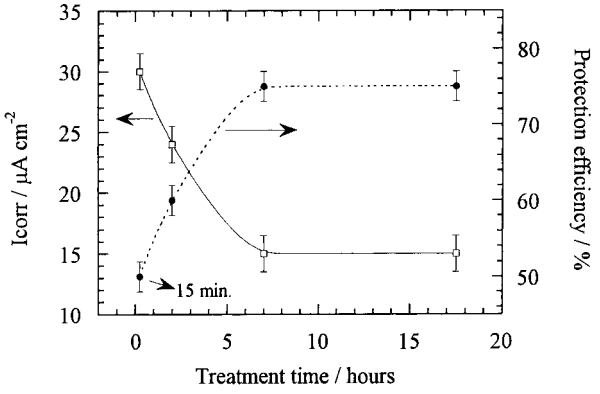

Fig. 3. Treatment time dependence of the corrosion current density (I_{corr}) and the protection efficiency (η) for samples treated at 25 °C in 2% CSN5 solution.

comparable to the protection performances estimated by Felloni et al. [23] who recorded polarization curves in 0.6 M NaCl aqueous medium for coatings obtained by treatment of zinc with chromate solutions; in this case η was 66%.

The protection efficiency (η) increased with immersion time as shown in Figure 3, which presents data for samples treated at 25 °C in 2% CSN5 solution, giving evidence of the progressive formation of a protective film on the electrode surface. After seven hours η was stabilized and reached 75%.

The effect of treatment bath pH on the performance of samples treated with 2% CSN5 solution (25 °C, 2 h) is illustrated in Figure 4. Satisfactory protection was obtained only for weakly acid pH values around 4. Similar behaviour was observed by Leroy [20] who related the strong peak in protection offered by aqueous solutions of 2,5-dimercapto-1,3,4-thiadiazole to zinc, to the incipient solubility of metal in the 4–6.5

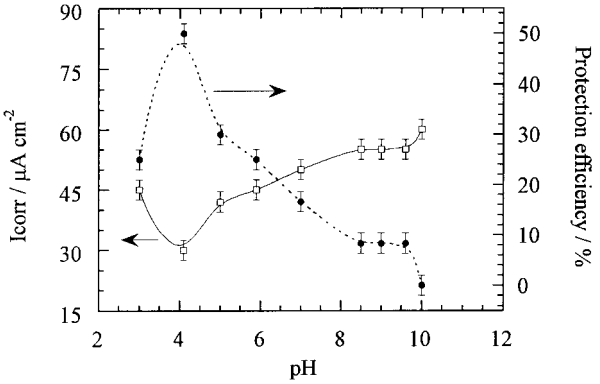

Fig. 4. Effect of the treatment bath pH on the corrosion current density (I_{corr}) and the protection efficiency (η) for samples treated at 25 °C in 2% CSN5 solution for 2 h.

pH range. In more alkaline solutions, extensive oxide or hydroxide formation occasions insufficient adhesion between the zinc and the organometallic film. In more acidic baths, the high dissolution rate of zinc hinders the formation of a protective layer on the electrode surface.

The electrochemical behavior of the treated samples depended strongly on the temperature of the treatment bath as shown in Figure 5(a), which gives the polarization curves of zinc treated for 2 h 30 min in 2% CSN5 solutions (pH 4.1). Both cathodic and anodic branches shifted towards lower current densities and their shape

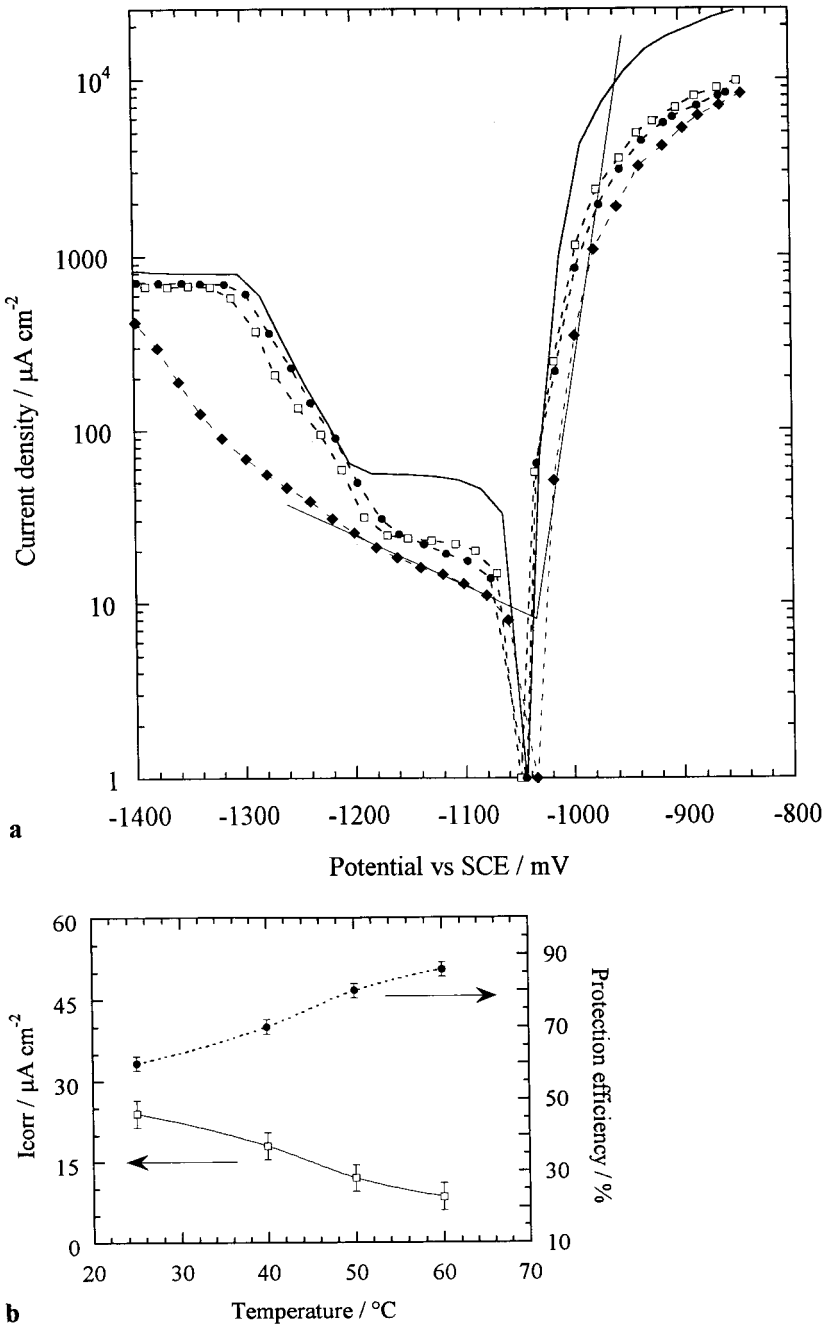

Fig. 5. (**a**) Polarization curves in aerated 0.2 M Na_2SO_4 + 0.2 M NaCl aqueous solution. Solid line: untreated zinc; broken lines: treated zinc (2% CSN5, 2 h 30 min, pH 4.1). Treatment bath temperature: (□) 40 °C; (●) 50 °C and (◆) 60 °C. (**b**) Temperature dependence of the corrosion current density (I_{corr}) and the protection efficiency (η).

changed appreciably especially above 50 °C. The protection offered by CSN5 was greatly enhanced and, in the case of 60 °C treatment, reached 86% (Figure 5(b)). The effect of temperature is believed to be related to an acceleration of the chemical reaction of organometallic complex formation on the zinc surface leading to a more homogenous protective layer.

3.2. *SEM-EDS examination*

To investigate the performance of the protective coating, a SEM study of zinc samples was carried out after recording the anodic polarization curve. While the untreated zinc appeared strongly corroded, in the case of treated samples no generalized attack was observed: the surface shows only a few pits covered with white corrosion products (Figure 6, *a*-region).

For untreated zinc the EDS spectrum indicated strong S and Cl peaks due to the corrosive agent (Figure 7(c)). For the treated zinc, analysis of the pit corrosion products showed these peaks greatly reduced (Figure 7(a)). Moreover, outside the pits, the Cl signal was practically undetected (Figure 7(b)); the observed sulfur signal originated from the organic molecules covering the zinc surface.

3.3. *XPS study*

XPS measurements were performed to study the film formed on the surface of a zinc specimen after immersion for 24 h 2% CSN5 solution (treatment bath temperature 25 °C, pH 4.1). Detailed information was also obtained from analysis of the Auger signal. The treated specimens were rinsed in ethanol for 20 s, washed with distilled water and dried in air, following which they were introduced into the ultrahigh vacuum.

Figure 8 allows the comparison of the Zn–LMM spectra of the untreated and treated zinc. The spectrum

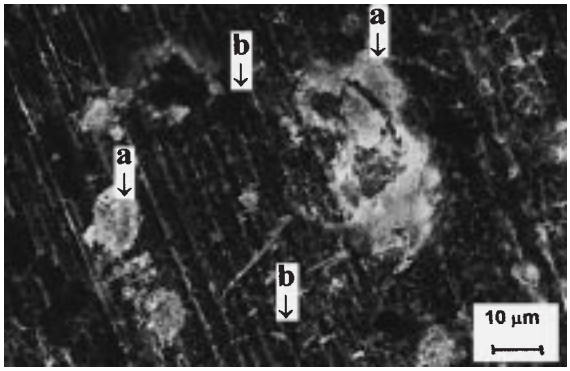

Fig. 6. SEM micrograph of treated zinc (2% CSN5, 24 h, 25 °C, pH 4.1) taken after anodic investigation in the corrosive medium.

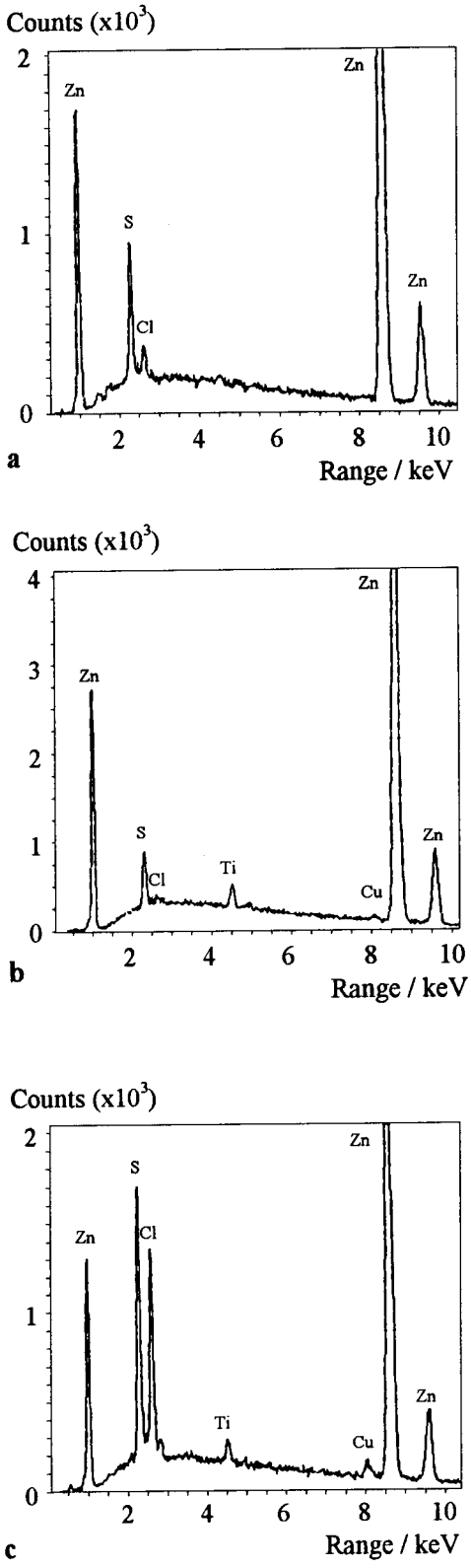

Fig. 7. EDS spectra of zinc surface after anodic investigation in the corrosion medium (**a, b**) respectively for *a* and *b* regions of Figure 6 (treated zinc); (**c**) for untreated zinc.

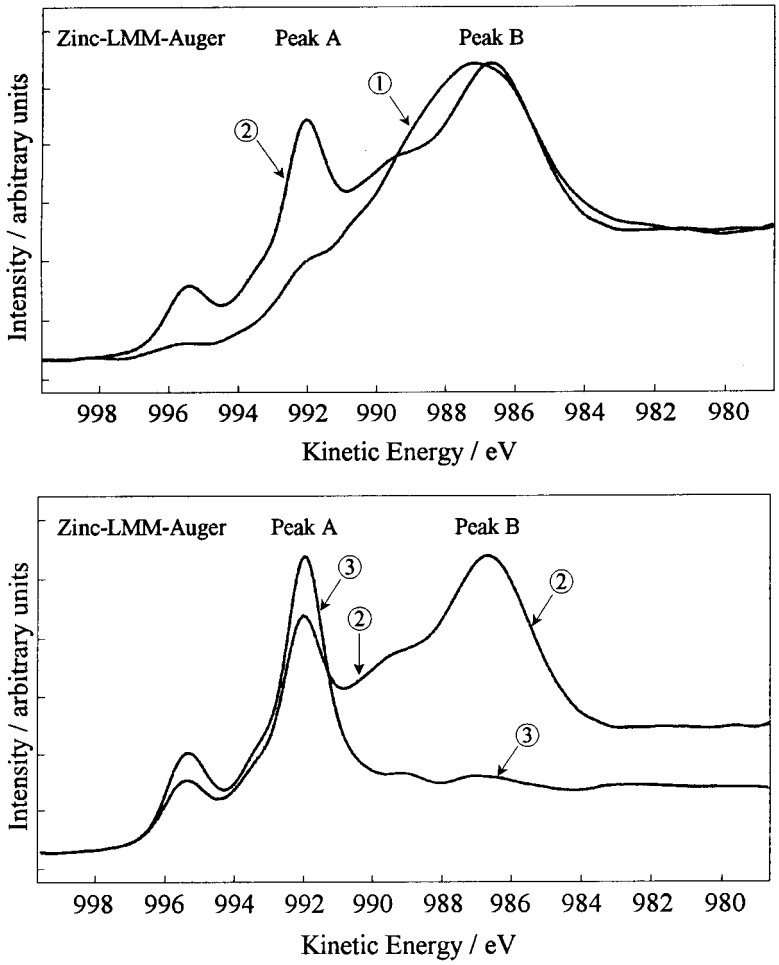

Fig. 8. Zn–LMM–Auger signal. Curves: (**1**) treated zinc (2% CSN5, 24 h, 25 °C, pH 4.1); (**2**) untreated zinc; and (**3**) untreated zinc after sputtering (10 min, 4 kV).

of the surface of the untreated zinc specimen (curve 1) shows two peaks: peak A at 992 eV was ascribed to the metallic zinc, whereas peak B at 986.5 eV to the zinc oxide formed naturally in air. For the untreated zinc this peak was removed after sputtering for 2 min with 2 kV argon ions (corresponding sputtering depth was ~20 Å) as shown in Figure 8, curve 3. In the case of treated zinc peak A was not observed (Figure 8, curve 2) indicating the presence of a thick protective layer which hindered the participation of the metallic zinc peak in the spectrum. Sputtering on this sample for 2 min, as well as for 8 min with 2 kV argon ions, did not affect the shape of peak B (not shown in Figure 8). These results along with the large structure of the peak B on the low kinetic energy side indicate the formation of new zinc bonds between the metal and the organic molecule, respectively.

The Zn $2p_{3/2}$ and Zn $2p_{1/2}$ peaks (Figure 9) for treated zinc also include two components which can be ascribed to zinc oxide (1023.2 and 1046.2 eV) and to the organometallic compound (1024.6 and 1047.7 eV). After sputtering for 1 min (2 kV) the ZnO-shoulders (Figure 9, curve 2) are almost removed. This superficial formation of zinc oxide could result from possible uncoated zones on the zinc surface.

The presence of the organic molecule on the zinc surface was also established by the strong nitrogen and sulfur peaks. XPS analysis in the N_{1s} region for the treated zinc (Figure 10, curve 1) exhibits an asymmetric peak with a shoulder on the low-energy side; these two components correspond to different N bonds. Comparison with the CSN5 powder spectrum (Figure 10, curve 2) which also presents the main peak but with a shoulder on the high-energy side, indicated that one of the two N atoms of the organic molecule was affected by new

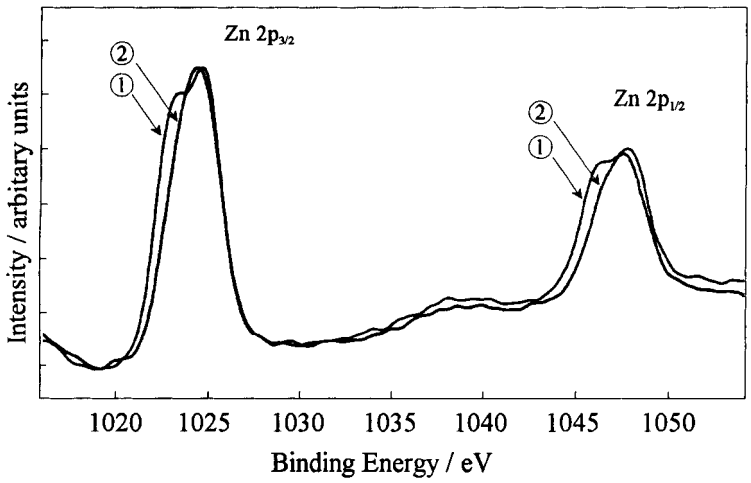

Fig. 9. Zn $2p_{3/2}$ – Zn $2p_{1/2}$ XPS spectra on the treated zinc (2% CSN5, 24 h, 25 °C, pH 4.1). (**1**) at the surface and (**2**) after sputtering (1 min, 2 kV).

chemical surroundings, probably because of the establishment of chemical bonds with the metallic zinc.

The great width of the S_{2p} peak for the coated specimen (Figure 11, curve 1) compared to that for CSN5 powder (Figure 11, curve 2) is difficult to explain, except by the presence of several components due to the participation of sulfur atoms in low energy bonds with the metallic zinc.

A number of subsequent sputterings on the treated zinc surface showed that a notable nitrogen and sulfur content persisted up to depth of about 100 Å giving an estimation of the thickness of the organometallic layer.

3.4. *FTIR study*

The FTIR spectrum of the organic molecule CSN5, obtained by transmission is presented in Figure 12(a). The characteristic bands at 3255.6 cm^{-1} and 3112.0 cm^{-1} were attributed to the stretching vibrations of the secondary amino —NH group [26]. These bands do not appear in Figure 12(b) which reports the FT reflection infrared spectrum of the zinc specimen treated for one day in solution containing 2% CSN5 (25 °C, pH 4.1). The vanishing of these bands indicates the deprotonation of the —NH group through the formation of chemical bonds between the organic compound and the metallic substrate.

The C=S band was difficult to identify because the carbon atom is linked directly to a nitrogen atom which induces coupling effects. In consequence, there are a number of different bands, each of which contains a contribution from the C=S stretching mode; the available data indicated a wide range of values concerning this band [27, 28]: 1480–1260 cm^{-1}, 1140–940 cm^{-1}, 800–600 cm^{-1}. The reflection spectrum of the zinc specimen treated with the inhibitor CSN5 (Figure 12(b))

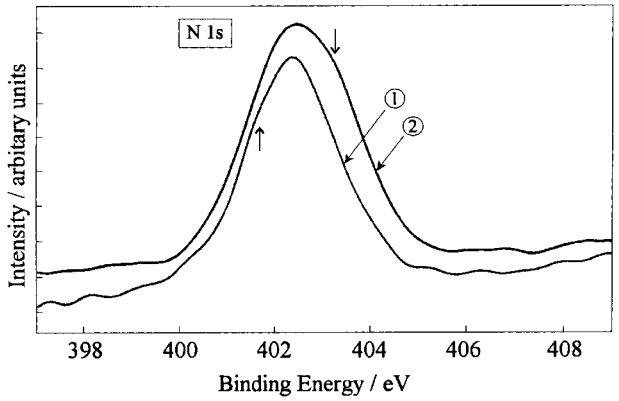

Fig. 10. N_{1s} XPS spectra. Curves: (**1**) - treated zinc (2% CSN5, 24 h, 25 °C, pH 4.1) and (**2**) CSN5 powder (pure).

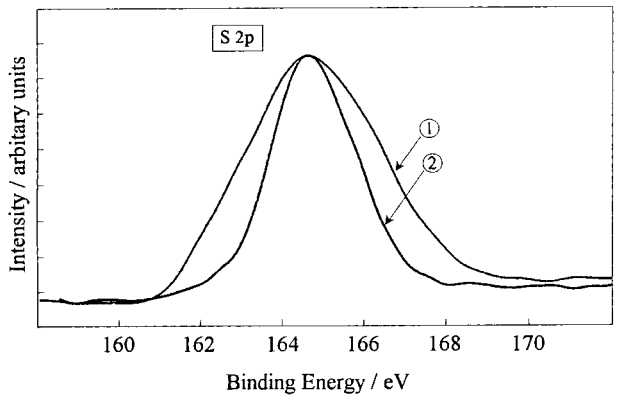

Fig. 11. S_{2p} XPS spectra. Curves: (**1**) treated zinc (2% CSN5, 24 h, 25 °C, pH 4.1) and (**2**) CSN5 powder (pure).

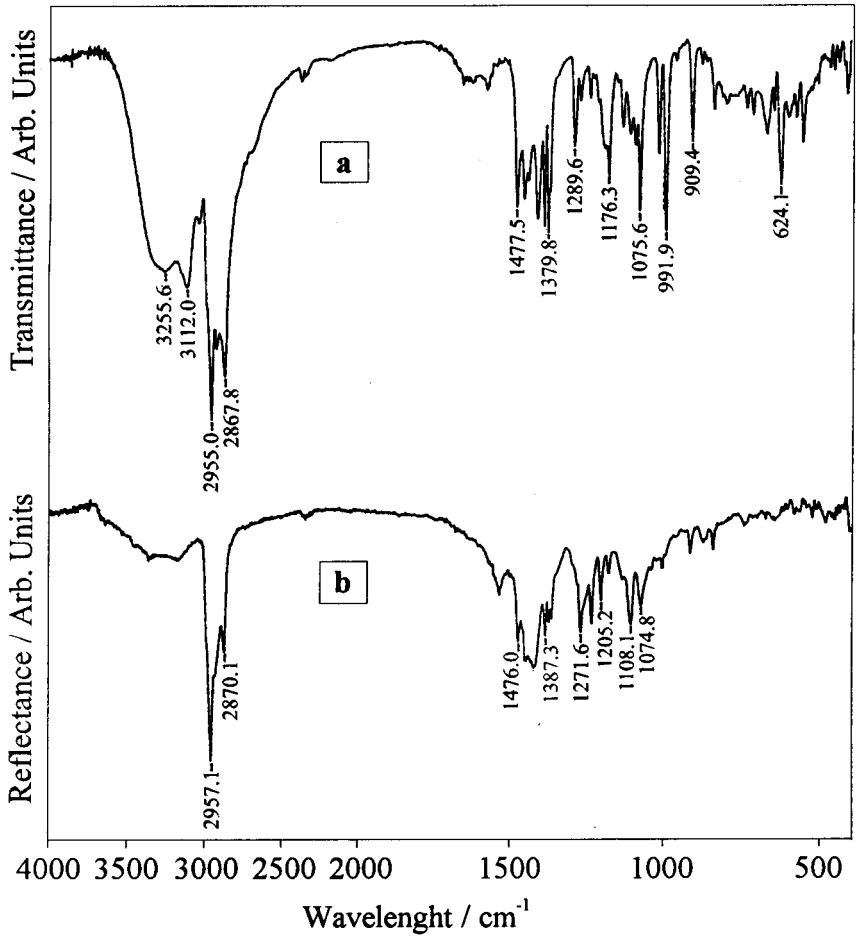

Fig. 12. FTIR spectra. (**a**) CSN5 powder in KBr pellet (transmission spectrum); (**b**) treated zinc (2% CSN5, 24 h, 25 °C, pH 4.1) (reflectance spectrum).

shows several modifications in these three domains especially the disappearance of the band at 624.1 cm^{-1}. These data indicate participation of the function C=S in molecule-substrate binding in accordance with the results of the XPS analysis.

The above observations lead to the conclusion that treatment of zinc in CSN5 solutions results in the formation of a Zn–CSN5 compound on the metal surface with a contribution of the deprotonated nitrogen and probably the sulfur atom. Taking into account the results of XPS as well as FTIR analysis, a chelate structure can be proposed with Zn–N and Zn–S bonds. However, the formation of a zinc complex cannot be excluded.

4. Conclusion

Electrochemical study showed that zinc treated beforehand with CSN5 has good corrosion resistance in aqueous chloride–sulfate solution. The observed protection was particularly affected by the pH and the temperature of the treatment bath: a maximum protection efficiency of about 90% was obtained at 60 °C and for weakly acid CSN5 solution (pH 4). The treatment induced a basic modification of the cathodic behaviour of zinc decreasing the electron transfer rate. The protection resulted from the formation of a stable organometallic film strongly attached to the zinc surface by the establishment of chemical bonds through the 5-thioxo 4-hydro 1H-pyrazole group of the CSN5 organic molecule involving the nitrogen of the secondary amino —NH group and probably the sulfur atom.

Acknowledgements

The assistance of M. Provencial and M. Chatainier with the XPS investigations is thankfully acknowledged. One

of the authors F. Noli would also like to thank the French Embassy in Athens for support during this work.

References

1. B.R.W. Hinton and L. Wilson, *Corros. Sci.* **29** (1989) 967.
2. M. Ihara, H. Nishihara and K. Aramaki, *Denki Kagaku* **60** (1992) 500.
3. C.M. Rangel, J. de Damborenea, A.I. de SA and M.H. Sewlicio, *Br. Corros. J.* **27** (1992) 207.
4. M.T. Makhlouf, A.A. Abdel-Hafez and S.A. Ibrahim, *J. Electrochem. Soc. India* **35** (1986) 89.
5. M.S. Abdel Aal, S. Radwan and A. El-Saied, *Br. Corros. J.* **8** (1983) 102.
6. M. Troquet, B. Laveissiere, J.P. Labbe and J. Pagetti, Proceedings of the 5th European Symposium on *Corrosion Inhibitors*, Ferrara, p. 921 (1980).
7. K. Wippermann, J.W. Schultze, R. Kessel and J. Penninger, *Corros. Sci.* **32** (1991) 205.
8. Awad I. Ahmed and S. Abdel-Hakam, *Anti-Corrosion*, **3** (1989) 4.
9. A.G. Gad Allah, M.M. Hefny, S.A. Salih and M. Sel-Basiouny, *Corrosion* **45** (1989) 574.
10. E. Stupnisek-Lisac and S. Podbrscek, *J. Appl. Electrochem.* **24** (1994) 779.
11. M. Troquet, J.P. Labbe and J. Pagetti, *Corros. Sci.* **21** (1981) 101.
12. S. Kawai, H. Kato and Y. Hayakama, *Denki Kagaku* **39** (1971) 288.
13. H. Konno, Z. Zhu and M. Nagayama, *Plat. Surf. Finish.* **74** (1987) 40.
14. E.E. Kriss, YU.I. Kuznetsov, I.G. Kuznetsova, L.P. Kazanskii, A.S. Grigorieva, N.F. Konakhovich and Yu.A. Fialkov, *Koord. Khim.* **11** (1985) 462.
15. B. Muller and G. Imblo, *Corros. Sci.* **38** (1996) 293.
16. B. Muller and I. Forster, *Corrosion* **52** (1996) 786.
17. V.T. Dorofeev, I.V. Volkov, O.P. Fedorkova and L.N. Shugurova, *Vopr. Khimii i Khim. Tekhnol.*, Khar'kov **77** (1985) 90.
18. C. Fiaud, S. Bensara, I. Demesy des Aulnois and M. Tzinmann, *Br. Corros. J.* **22** (1987) 102.
19. R.L. Leroy, *Mater. Perform.* **19** (1980) 54.
20. R.L. Leroy, *Corrosion* **34** (1978) 98.
21. R.L. Leroy, *Corrosion* **34** (1978) 113.
22. R.L. Leroy and Z. Zavorski, *Corros. Sci.* **17** (1977) 943.
23. L. Felloni, R. Fratesi, G. Roventi and L. Fedrizzi, Proceedings of the 11th International Corrosion Congress, Florence, Italy, 2–6 April 1990 (edited by A.I.M., Milan), vol.2, p.365.
24. C. Deslouis, M. Duprat and C. Tournillon, *J. Electroanal. Chem.* **181** (1984) 119.
25. C. Deslouis, M. Duprat and C. Tournillon, *Corros. Sci.* **29** (1989) 13.
26. A.M. Lamazouère, *Thesis*, Université Paul Sabatier, Toulouse (1972).
27. L.J. Bellamy, *The Infrared Spectra of Complex Molecules*, Chapman & Hall, London (1975).
28. L.J. Bellamy, *Advances in Infrared Group Frequencies*, Chapman & Hall, London (1980).